Development of a Cold Field-Emission Gun for a 200kV Atomic Resolution Electron Microscope

Yuji Kohno,[1] Eiji Okunishi,[1] Takeshi Tomita,[1] Isamu Ishikawa,[1] Toshikatsu Kaneyama,[1] Yoshihiro Ohkura,[1] Yukihito Kondo[1] and Thomas Isabell.[2] 1. JEOL Ltd., Akishima, Tokyo, Japan. 2. JEOL USA Inc., Peabody, Boston, MA, USA.

BIOGRAPHY

Yuji Kohno has a master's degree in particle physics from Kyoto University. He has been with JEOL for five years. He is now in charge of developing electron sources for transmission electron microscopes.

ABSTRACT

We have developed a new type of cold field-emission electron gun (CFEG) for a 200 kV scanning transmission electron microscope, the JEM-ARM200F. This CFEG provides a newly developed vacuum system which can evacuate the area around the tip to the order of 10^{-9} Pa resulting in good stability of emission. The CFEG is thus able to produce high brightness, a small energy spread and stable emission all at the same time. The low chromatic aberration from the small energy spread (0.32 eV FWHM) improves the resolution of Cs-corrected STEM. Additionally, the small probe with its high current and small energy spread enables high-speed acquisition and high spatial and energy resolution in electron energy-loss spectroscopy. In this article we describe the design of the new CFEG and demonstrate that at 200 kV the 63 pm dumbbell of GaN (211) can be resolved and that EELS analysis with a resolution of better than 0.3 eV reveals the fine structure of the titanium $L_{2,3}$ edge.

KEYWORDS

scanning transmission electron microscopy, electron energy-loss electron microscopy, high angle annular darkfield, aberration correction, cold field-emission gun, atomic resolution, semiconductors

AUTHOR DETAILS

Mr Yuji Kohno,
JEOL Ltd,
1-2 Musashino 3-chome,
Akishima, Tokyo, Japan
Tel +81 42 542 2227
Email: yukohno@jeol.co.jp

Microscopy and Analysis 24(7):S9-S13 (AM), 2010

INTRODUCTION

Recent electron optical technology makes it possible to correct the spherical aberration [1] that used to be the main obstacle limiting the probe size in scanning transmission electron microscopy (STEM). The advantages of this technology have been proven by fruitful results in both imaging [2,3] and analysis [4,5]. Because the spherical aberration can be corrected, efforts are now directed towards the reduction of the chromatic aberration. Since the chromatic aberration is proportional to the energy spread of the electron source, a low energy spread further reduces the probe size of a STEM spherical aberration-corrected column. At the same time, the lower energy spread is useful for higher energy-resolution analysis in electron energy-loss spectroscopy (EELS).

A cold field-emission electron gun (CFEG) using a sharpened tungsten tip is known to create an electron source with a low energy spread as well as high brightness. These characteristics give high speed acquisition with high spatial and energy resolution in STEM and EELS, as shown by many results from Cs-corrected machines [6-8] as well as instruments without Cs correction [9]. However, the CFEG source has some difficulties in emission stability. It is well known that residual gases around the tip degrade the emission stability of a CFEG. The work function is changed by the adsorption of gases, resulting in a decrease of the emission current. Furthermore, the fluctuation of the adsorbate and the sputtering of the tip by ionized gases cause emission noise [10].

Therefore we have developed a new type of CFEG for a 200 kV electron microscope, the JEM-ARM200F (Figure 1). This CFEG has a newly developed vacuum system, which can evacuate the area around the tip to the order of 10^{-9} Pa, resulting in improved stability of the emission current. This paper reports the results of the performance of the new CFEG on the JEM-ARM200F equipped with a STEM Cs corrector and an electron energy-loss spectrometer (Gatan GIF Quantum).

STABILITY OF THE EMISSION

Figure 2 shows a schematic of the vacuum system [11]. Three 100 L s^{-1} non evaporable Getter pumps (NEG) (SAES Getters) and a 200 L s^{-1} noble ion pump are used to evacuate the emitter chamber. To isolate the vacuum of the gun chamber from the column a differential pumping system is employed. This is achieved by the insertion of two intermediate chambers between the gun and column chambers. This system achieves a vacuum of less than 5 x 10^{-9} Pa at the bottom of the accelerating tube, as measured by the extractor gauge. Simulated calculation estimates the pressure around the tip to be 1 x 10^{-9} Pa. This value is attained because the NEG is placed near the tip and its vacuum conductance is high.

Figure 3 shows the drift of the emission and probe currents after flashing. The probe current, at a level commonly used for imaging and analysis, gradually decreases by 10% over 2 hours. It is stable enough to start observation and analysis almost immediately after flashing. This is difficult for an ordinary CFEG operated at vacuum on the order of 10^{-8} Pa, where users typically have to wait for several tens of minutes to have a stable emission current.

ENERGY SPREAD OF THE CFEG

The energy spreads of the CFE and Schottky guns are compared in Figure 4. A 12 μA emission current with the CFEG gives the same probe current as commonly used with the Schottky gun, and the full width at half maximum (FWHM) of the energy spread at this condition for the CFEG is 0.42 eV. Thus, the FWHM for the CFEG is nearly half that of the Schottky (0.7 eV) with the same probe current. The energy spreads for low and high current conditions are shown in Figure 4 and are 0.26 eV

Figure 1:
The new cold field-emission gun on the JEOL JEM-ARM200F.

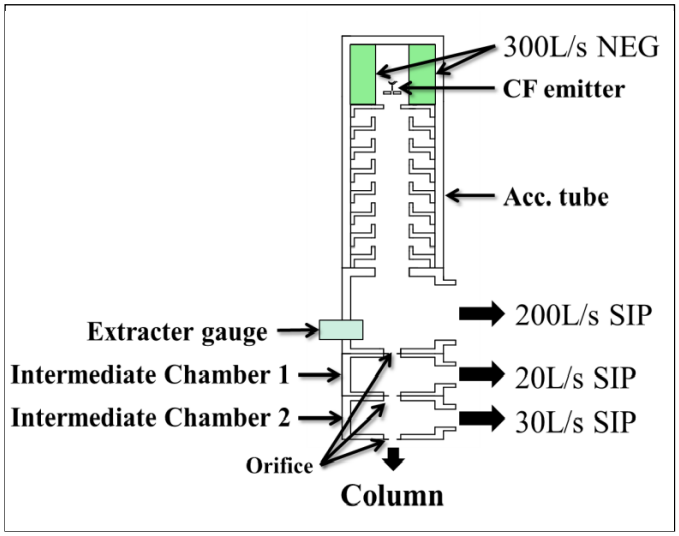

Figure 2:
Schematic of the new vacuum system in the CFEG.

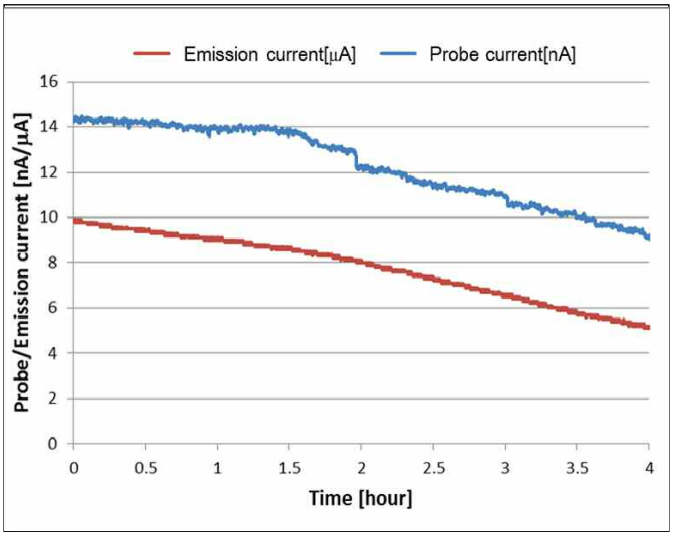

Figure 3:
Drift of the probe (blue) and emission (red) currents after flashing.

and 0.51 eV respectively. The increase of the FWHM is nearly proportional to the emission current, due to the statistical Coulomb effect [12]. The lowest value of 0.26 eV is close to the theoretical value 0.22 eV at the emitter surface. This shows that the high-voltage stability is high enough to maintain the energy spread of the CFEG.

HIGH-RESOLUTION STEM IMAGING

The probe size of a STEM Cs-corrected TEM is determined by diffraction and the chromatic aberration. The beam spreading by chromatic aberration d_c is given by:

$$d_c = C_c\,(dE/E)\,\alpha$$

where C_c is the coefficient of chromatic aberration, dE is the energy spread, E is the accelerating voltage and α is the convergence semi angle.

The beam spreading by diffraction aberration is given by the radius of the Airy disc r_A :

$$r_A = 0.61\lambda/\alpha$$

where λ is the wavelength of the electron beam. There exists an optimum α where the sum of these two aberrations is at a minimum. If we obtain a smaller chromatic aberration by the smaller dE of the CFEG, the optimum α becomes larger resulting in a smaller diffraction aberration.

Figure 5a shows a raw high-angle annular dark field (HAADF) STEM image of GaN (211) at 200 kV. The 63 pm spacing between Ga-to-Ga in each dumbbell was well resolved in the intensity profile shown in Figure 5c. The Fourier transform (Figure 5b) clearly shows the information transfer to 63 pm which corresponds to this dumbbell spacing. The convergence semi angle is 29 mrad, which is experimentally confirmed to be optimum and is larger than that of the Schottky case (23 mrad). This indicates that the reduction in chromatic aberration contributes to an improved probe size.

The effect of the chromatic aberration becomes more important at lower accelerating voltages, because the ratio dE/E becomes larger. Therefore, the narrow energy spread of the CFEG has an advantage for low acceler-

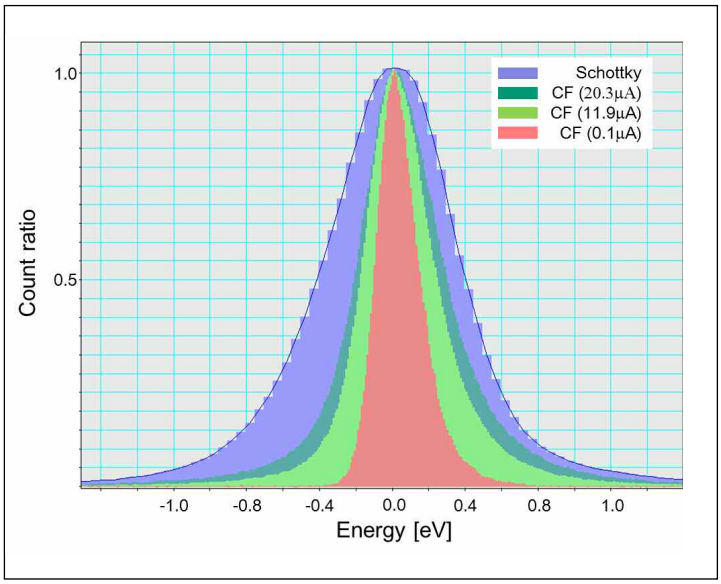

Figure 4:
The energy spread of the CFE and Schottky guns.

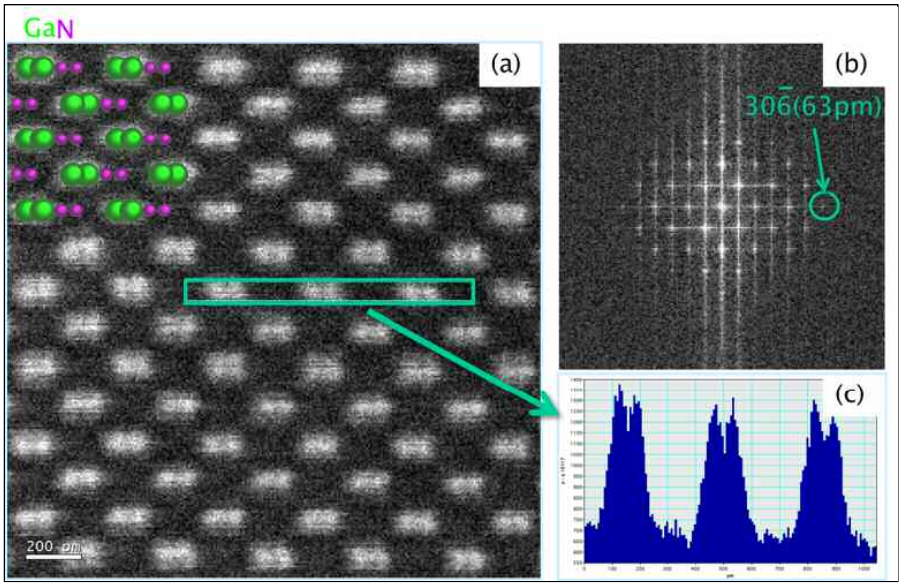

Figure 5:
(a) A raw HAADF STEM image of GaN (211) taken at 200 kV. The spacing between Ga-to-Ga is 63 pm. (b) The Fourier transform of the raw image shows 306 spot which corresponds 63 pm. (c) The intensity profile of the indicated rectangular region in the raw image shows that the dumbbells are well resolved.

ating voltage observation. Figure 6 shows the HAADF STEM image of Si (110) at 80 kV.

ELECTRON ENERGY-LOSS SPECTROSCOPY ANALYSIS

The small intense probe from the high brightness CFEG source serves well for high resolution EELS analysis. Figure 7a shows a plot of the diffraction spots of the highest frequencies in the Fourier transform for a series of HAADF STEM images taken at different probe currents, using a Si (110) sample. Figure 7b is an example of the Fourier transform. The red plot is acquired with an energy spread 0.51 eV and blue plot at 0.32 eV. Information of less than 200 pm can be transferred to STEM HAADF images acquired with a probe current of 2000 pA.

These small probes with high current and small energy spread provide high-speed EELS acquisition with high spatial and energy resolution. Figure 8 shows the results of a 64-by-64 pixel STEM EELS spectrum image (SI) of $SrTiO_3$ (100). Figure 8c shows the spectrum of a single Ti + O site extracted from the SI. The data cube of the SI was acquired under the conditions: probe current of 280 pA, energy spread of 0.4 eV, dispersion of spectrometer of 0.2 eV per channel, and an exposure time of 10 ms per pixel. The total time needed to acquire these spectrum images was 240 seconds. Figures 8b, 8d, 8e and 8f show a series of elemental maps of $SrTiO_3$. Figure 8a shows a STEM HAADF image. All the spectrum images show a clear separation of the composing elements.

CONCLUSIONS

We have developed a new CFEG that realizes high brightness and a low energy spread with stable emission. The small chromatic aberration due to the low energy spread improves the resolution of Cs-corrected STEM. We have demonstrated that the 63 pm dumbbell of GaN (211) can be resolved at 200 kV.

We conclude that the present CFEG with good stability realizes sub-Angstrom STEM imaging with high energy resolution analysis of better than 0.3 eV. In spite of the short acquisition time and large dispersion, a spectrum shown in Figure 8c has high signal-to-noise ratio, which shows the fine structure of the titanium $L_{2,3}$ edge.

REFERENCES

1. Haider, M. et al. Nature 392:768, 1998.
2. Sawada, H. et al. J. Electron Microscopy 54:123, 2005.
3. Erni, R. et al. Phys. Rev. Lett. 102:096101, 2009.
4. Okunishi, E. et al. Microsc. Microanal. 12(Suppl 2):1150, 2006.
5. Bosman, M. et al. Phys. Rev. Lett. 99:086102, 2007.
6. Sawada, S. et al. J. Electron Microscopy 58:357, 2009.
7. H. Sawada, H. et al. JJAP 46:568, 2007.
8. Nellist, P. D. et al. Science 305:1741, 2004.
9. Kimoto, K. et al. Science 450:702, 2007.
10. Yeong, K. S., Thong, J. T. L. J. Appl. Phys. 99:104903-1, 2006.
11. Tomita, T. et al. Microsc. Microanal. 15(Suppl 2):1084, 2009.
12. Jansen. G. H. Coulomb interaction in particle beams. Academic Press 1990.

©2010 John Wiley & Sons, Ltd

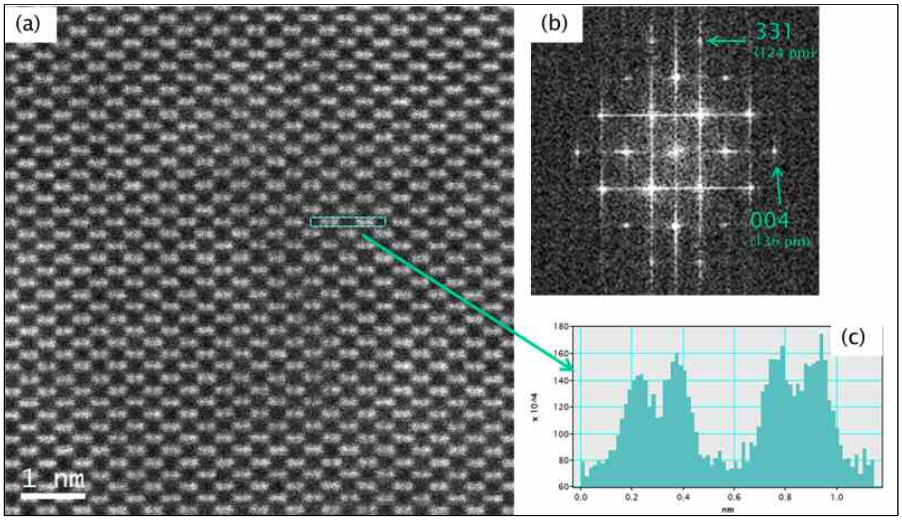

Figure 6:
(a) A raw HAADF STEM image of Si (110) at 80 kV. (b) The Fourier transform of the image shows the 331 spot corre-sponds to 124 pm. (c) The intensity profile shows that the 136 pm spacing is resolved.

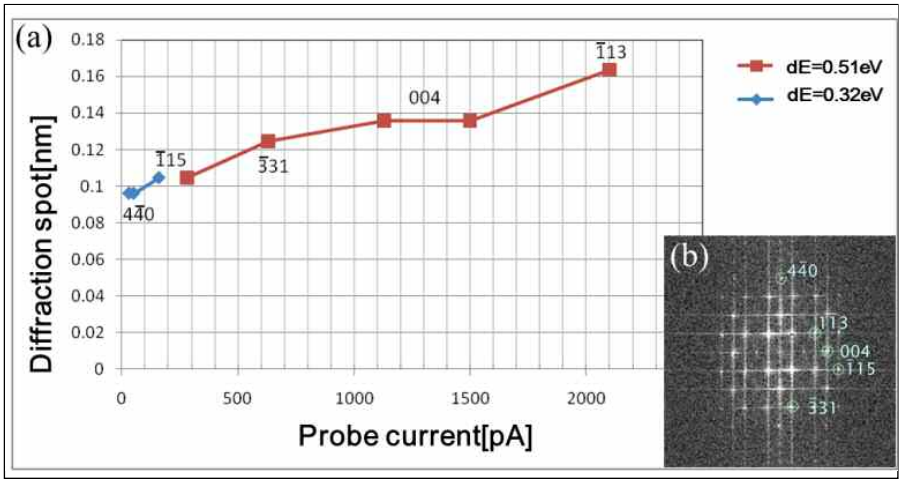

Figure 7:
(a) A plot of diffraction spots of the highest frequencies in the Fourier transform for a series of Si (110) HAADF STEM images taken with different probe currents. (b) A Fourier transform of an HAADF STEM image of Si (110) acquired with probe current of 30 pA and dE of 0.32 eV.

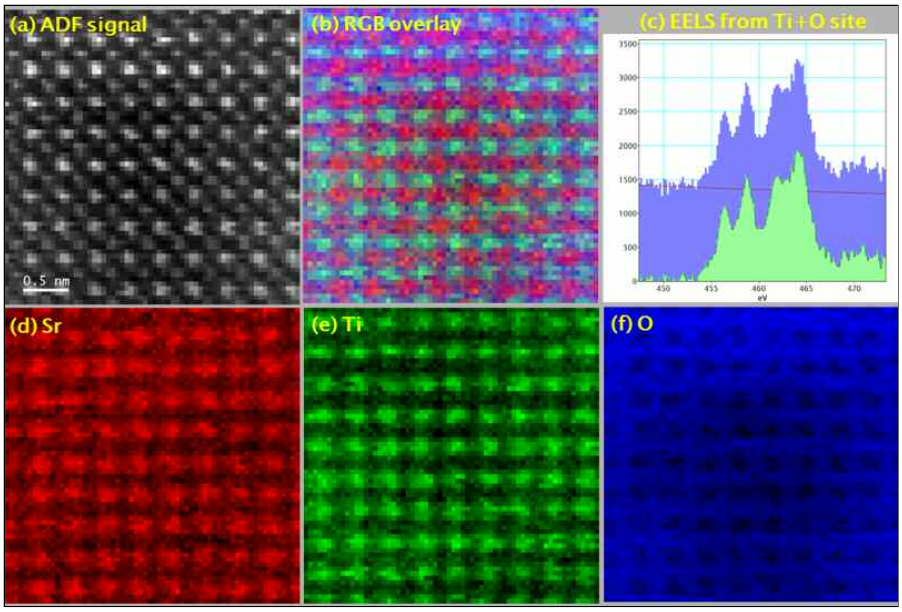

Figure 8:
(a) A STEM HAADF image obtained simultaneously. (b, d, e and f) A series of elemental maps of $SrTiO_3$ reconstructed from a data cube of a spectrum image. (c) Spectra of a single Ti + O site extracted from the data cube. Upper and lower images are unprocessed and background subtracted.